

CHEMICAL ELEMENTS AT HIGH AND LOW REDSHIFTS

MAX PETTINI

Institute of Astronomy, Cambridge, CB3 0HA, England

Abstract. The past few years have seen a steady progress in the determination of element abundances at high redshifts, with new and more accurate measures of metallicities in star-forming galaxies, in QSO absorbers, and in the intergalactic medium. We have also become more aware of the limitations of the tools at our disposal in such endeavours. I summarise these recent developments and—in tune with the theme of this meeting—consider the clues which chemical abundance studies offer to the links between the high redshift galaxy populations and today’s galaxies. The new data are ‘fleshing out’ the overall picture of element abundances at redshifts $z = 2 - 3$ which has been gradually coming into focus over the last decade. In particular, we can now account for at least 40% of the metals produced by the global star formation activity in the universe from the Big Bang to $z = 2.5$, and we have strong indications of where the remainder are likely to be found.

1 Introduction

Studies of element abundances, like many other areas of astrophysics, have undergone a remarkable acceleration in the flow of data over the last few years. We have witnessed wholesale abundance determinations in tens of thousands of galaxies from large scale surveys such as the 2dF galaxy redshift survey and the Sloan Digital Sky Survey (SDSS), measurements of the abundances of different elements in individual stars of Local Group galaxies beyond the immediate vicinity of the Milky Way, and the determination with exquisite precision of the detailed chemical composition of some of the first stars to form in the Galactic halo, with less than one thousandth of the heavy elements which were present when the Sun formed. Chemical abundance studies are also increasingly being extended to high redshifts, charting the progress of stellar nucleosynthesis over most of the age of the universe. These are all projects which were well beyond our capabilities only a decade ago.

The main motivation common to all of these observational efforts is to use the chemical information as one of the means at our disposal to link the properties of high redshift galaxies with those we see around us today and thereby understand the physical processes at play in the formation and the evolution of galaxies. This is indeed the theme which has inspired this meeting. Viewed from this perspective, the remarkable observational advances of the last few years have yet ‘to deliver’ fully. That is, we are still struggling to understand and fit together into a coherent picture of the chemical evolution of galaxies all this new information which we have been gathering at such a fast pace. It is this effort which will be the main focus of my review, which I have divided into four parts.

First I shall review the tools at our disposal for measuring element abundances, which themselves are far from being firmly established and calibrated, but rather have been undergoing significant scrutiny and revisions of late. Second, I shall present recent results on element abundances at high redshift in star-forming galaxies and in QSO absorption line systems. I shall then consider the clues which these measurements offer us in our quest to establish a connection between these high redshift populations and their descendants in today’s universe. The review concludes with an overall assessment of our knowledge of element abundances in different components of the universe at $z = 2.5$ and their evolution to the present time.

2 Abundance Measurement Techniques: Recent Developments

2.1 Emission Line Abundances

Nebular emission lines from H II regions have been the main tool at our disposal for measuring element abundances, and their radial gradients, in low redshift galaxies. In general, one has to rely on some empirical calibration of the strongest emission lines which are the ones most easily observed. Much work has been devoted to these calibrations in recent years, but there is still significant dispersion in the metallicities implied by different indices and, more worryingly, between different calibrations of the same index.

Recently, using large aperture telescopes, it has become possible to detect weak, temperature sensitive, auroral lines in extragalactic metal-rich H II regions (e.g. Garnett, Bresolin, & Kennicutt 2004). These lines should, at least in principle, allow an accurate measure of the temperature of the H II regions studied and thereby put the abundance determinations on a more solid footing. The results so far (several groups are now involved in this type of work—see also Sara Ellison’s contribution to these proceedings) suggest that the well-used $R23$

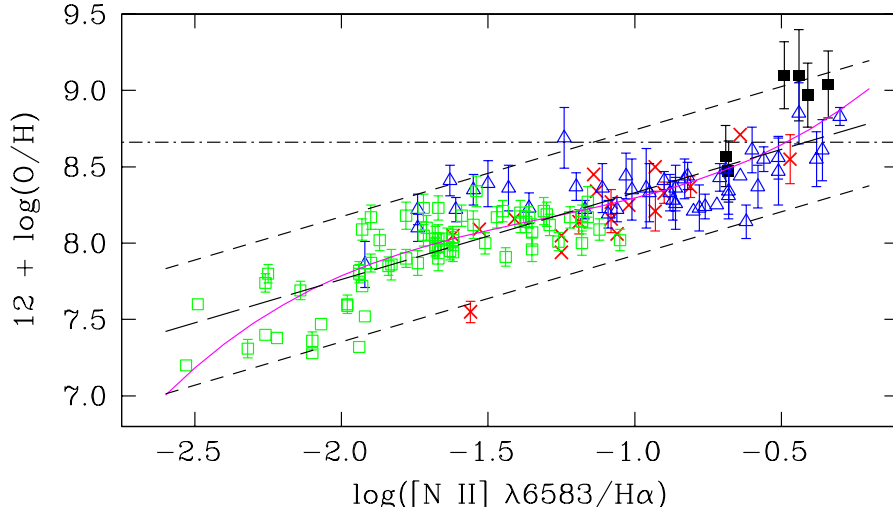


Figure 1: The empirical calibration by Pettini & Pagel (2004) of the $N2$ index, defined as $\log([N \text{ II}] \lambda 6583/H\alpha)$. Symbols are for individual H II regions with measured electron temperature or where the oxygen abundance has been derived with detailed photoionisation models—see Pettini & Pagel (2004) for references to the original works. The long-dash line is the best fitting linear relationship: $12+\log(O/H) = 8.90+0.57 \times N2$. The short-dash lines encompass 95% of the measurements and correspond to a range in $\log(O/H) = \pm 0.41$ relative to this linear fit. The continuous line is a cubic function of the form $12+\log(O/H) = 9.37+2.03 \times N2+1.26 \times N2^2+0.32 \times N2^3$ which, however, gives only a slightly better fit to the data (95% of the data points are within ± 0.38 of this line). The dot-dash horizontal line shows the solar oxygen abundance $12 + \log(O/H) = 8.66$ (Asplund et al. 2004).

index of Pagel et al. (1979) may overestimate the oxygen abundance significantly at high metallicities—and in case you should think that high metallicities are not relevant at high redshifts, think again! There is still a degree of controversy as to what extent these temperature-based abundances should be trusted (e.g. Stasińska 2005). If confirmed by future work, the implications of these initial studies are profound: super-solar metallicities are much rarer than previously envisaged (which may be in better accord with the predictions of chemical evolution models and with the paucity of super-metal-rich stars in the inner regions of the Milky Way) and galactic abundance gradients are more shallow than we were led to believe.

When it comes to applying these line diagnostics at high redshifts we are faced with additional problems, apart from the obvious one of a reduction in the flux received. When the emission lines are redshifted to near-infrared wavelengths only a subset of the strong lines is normally accessible, free from water vapour absorption and OH emission from the night sky. Even at the highly convenient redshift of $z \simeq 2.3$, where all the strong lines fall into near-IR windows, there is at present only one near-IR spectrograph on a large telescope, the Gemini GNIRS, which allows one to record all the strong lines, from $[O \text{ II}] \lambda 3727$ to $H\alpha$ and $[S \text{ II}] \lambda \lambda 6716, 6731$, simultaneously. For this reason, an abundance index based on the ratio of only two lines which are close in wavelength is particularly attractive. Despite concerns about its dependence on the ionisation parameter, the $N2$ index (see Figure 1) recently recalibrated by Pettini & Pagel (2004) has so far proved to be the most direct way to obtain at least an approximate estimate of the degree of metal enrichment of star-forming galaxies at $z = 1.5 - 2.5$.

2.2 Absorption Line Abundances

Resonance absorption lines in the rest frame ultraviolet are the main tool at our disposal for determining the abundances of a wide variety of chemical elements in cool interstellar gas. They have been applied primarily to the interstellar medium (ISM) of the Milky Way and Magellanic Clouds, and to high redshift absorption systems seen in the spectra of QSOs. This technique is capable of achieving high precision, provided one is in a regime where the absorption line optical depth is low (i.e. line saturation is not a concern), ionisation corrections are negligible, and dust depletions can be accounted for. These are all tractable problems in damped Lyman α systems (DLAs), the class of QSO absorbers with the largest column densities of neutral gas (Wolfe, Prochaska, & Gawiser 2005). However, this is generally *not* the case in star-forming galaxies at high z , where normally: (i) only the strongest (and therefore saturated) lines are measured; (ii) $N(\text{H I})$ is unavailable (given that the Ly α line is a complex blend of emission and absorption); (iii) the spectrum is a composite of multiple sightlines, so that there may be issues of non-uniform coverage of the background source against which the absorption lines are detected; and (d) the ionisation structure of the ISM is likely to be far from simple.

2.3 Stellar Abundance Diagnostics

The UV spectra of star-forming galaxies are rich in stellar features, including photospheric lines and P-Cygni features produced in the outflowing winds of the most luminous stars. Given the difficulties with the interstellar absorption lines outlined above, attention has turned to the stellar spectrum in the search for useful abundance diagnostics (e.g. Leitherer et al. 2001). The sophistication of modern non-LTE, line blanketed, stellar atmosphere codes, such as *WM-basic* (Pauldrach et al. 2001), and of stellar population spectral synthesis codes, such as *Starburst99* (Leitherer et al. 1999), allowed Rix et al. (2004) to fully synthesise the emergent spectrum of a star-forming galaxy for a variety of star formation histories and metallicities. As expected, it is the wind lines—particularly Si IV $\lambda\lambda 1393, 1402$ and C IV $\lambda\lambda 1548, 1550$ —which respond most sensitively to metallicity. In practice, however, these resonance lines are usually blended with strong interstellar components in the spectra of starburst galaxies, near and far, so that their measurement is not straightforward. Rix et al. (2004) also quantified the dependence on metallicity of a number of blends of stellar photospheric lines, particularly a broad feature due to Fe III at wavelengths between 1880 and 2020 Å (see Figure 2). Their main conclusion is that these features can indeed be calibrated against metallicity Z , although their broad and shallow nature requires spectra of higher signal-to-noise ratio (S/N) than that normally afforded by current instrumentation. Thus, while at present UV stellar features provide mostly a consistency check on other, more straightforward, metallicity indicators, I expect them to play a more important role in chemical abundance studies in the future, when the next generation of very large telescopes will routinely give us good quality spectra of high redshift galaxies.

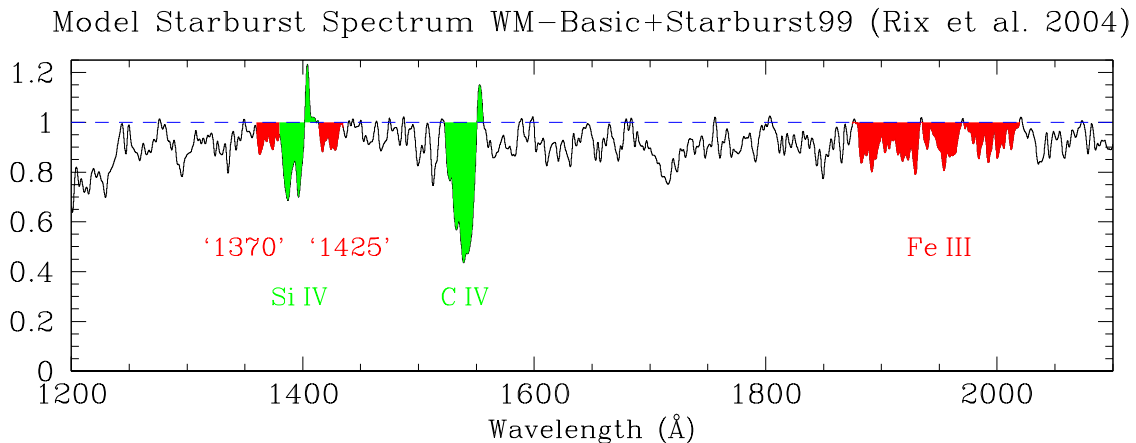


Figure 2: Fully theoretical UV spectrum of a starburst galaxy computed by Rix et al. (2004) for the case of continuous star formation with a Salpeter initial mass function (IMF) and solar metallicity. The shaded regions indicate wind lines (green) and blends of photospheric lines (red) found by Rix et al. to be sensitive to metallicity.

3 Abundance Measurements: Recent Results

3.1 Star-Forming Galaxies

The largest sample of high redshift galaxies with abundance determinations consists of nearly 100 UV-selected galaxies at redshifts $z \simeq 2.2$ satisfying the ‘BX’ colour criteria of Adelberger et al. (2004), and whose general properties have been described by Steidel et al. (2004). Erb et al. (2006a,b) used the near-infrared spectrograph NIRSPEC on the Keck II telescope in the K -band to record the spectral region encompassing the H α emission line and constructed composite spectra of sufficiently high signal-to-noise ratio to allow the weaker [N II] (and [S II]) emission lines to be measured. Application of the $N2$ index calibration of Pettini & Pagel (2004) then yields average values of the oxygen abundance for different subsets of these galaxies. Two examples are shown in Figure 3, constructed from galaxies respectively brighter and fainter than $K_s = 20$; the former exhibit approximately solar (O/H) and even in the fainter ones the average metallicity is only a factor of ~ 2 below solar (Shapley et al. 2004). A clearer pattern emerges when bins in stellar mass are considered: Erb et al. (2006a) found that galaxies which are young and have turned only a small fraction of their baryons into stars have (O/H) $< 1/3$ solar, while in galaxies which have already assembled $\sim 10^{11} M_\odot$ in stars (and galaxies with $K_s < 20$ tend to be mostly in this category) the oxygen abundance is close to solar.

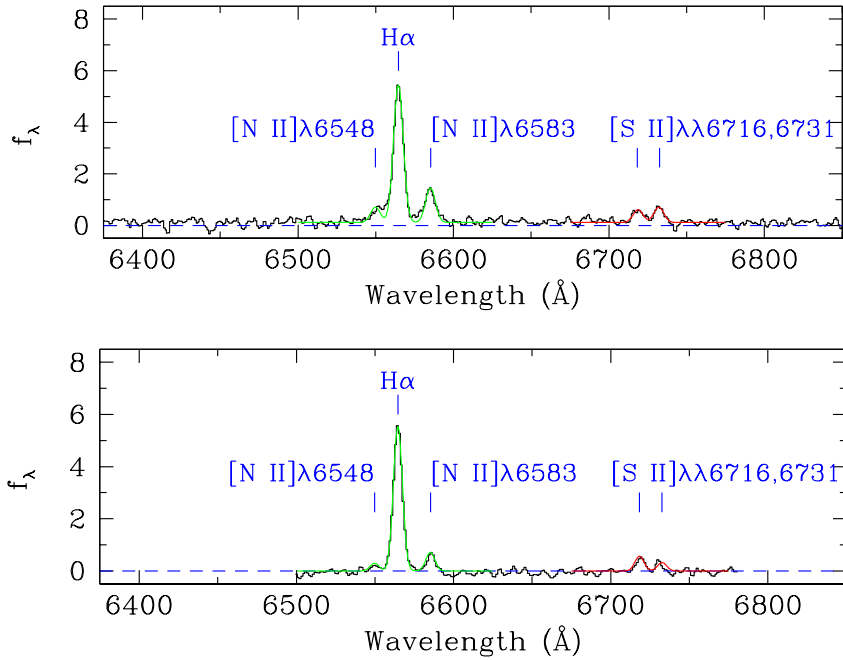


Figure 3: Composite spectra of BX galaxies at $z \simeq 2.2$ from the survey by Erb et al. (2006b). *Upper Panel:* galaxies brighter than $K_s = 20$ have a mean ratio $[\text{N II}]/\text{H}\alpha = 0.25$ which indicates an oxygen abundance $12 + \log(\text{O}/\text{H}) = 8.56$, or $\sim 4/5$ solar, if the local calibration of the $N2$ index with (O/H) applies to these galaxies. *Lower Panel:* galaxies fainter than $K_s = 20$ have $[\text{N II}]/\text{H}\alpha = 0.13$ and $12 + \log(\text{O}/\text{H}) = 8.39$ or $\sim 1/2$ solar.

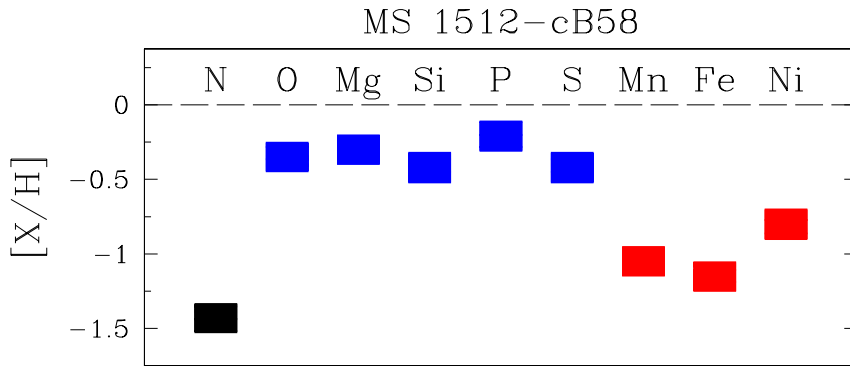


Figure 4: Element abundances in the ambient interstellar medium of the Lyman break galaxy MS 1512-cB58, at $z = 2.7276$, determined by Pettini et al. (2002). I use the conventional shorthand whereby $[\text{X}/\text{H}]_{\text{cB58}} = \log(\text{X}/\text{H})_{\text{cB58}} - \log(\text{X}/\text{H})_{\odot}$. While O and other α -capture elements (blue rectangles) have already reached $\sim 2/5$ of their solar values, the production and mixing within the ISM of Fe-peak (red) and N (black) apparently lag behind (even when account is taken of likely dust depletions). If N is produced mostly by stars in the mass range $3 - 7M_{\odot}$, the implied timescale for the metal enrichment of the ISM is very rapid, only a few hundred million years (Matteucci & Pipino 2002). MS 1512-cB58 is still the only high redshift galaxy where this type of refined abundance analysis has been possible, thanks to gravitational lensing by a foreground galaxy cluster which magnifies the signal by a factor of ~ 25 .

The conclusion that many star-forming galaxies had already gained near-solar metallicities at $z = 2 - 3$, while perhaps surprising to some, has in fact been reached independently by several groups applying different abundance diagnostics (some more reliable than others) to galaxies selected by different techniques, including near-IR and sub-mm selection (e.g. Mehlert et al. 2002; Savaglio et al. 2004; de Mello et al. 2004; Swinbank et al. 2004). In all of these cases, however, we are dealing with relatively bright objects, more luminous than $\sim 1/4L^*$. While the work of Erb et al. (2006a) has shown that there is no clear luminosity-metallicity relation in these galaxies—given the wide spread in their mass-to-light ratios even at rest frame near-IR wavelengths (Shapley et al. 2005)—it is still likely that galaxies with luminosities $L \ll L^*$ are in general less chemically enriched.

The ‘metallicity’ deduced by all of the above studies is only a rough measure of the overall degree of metal enrichment of the galaxies considered. Much more information is potentially available from their detailed chemical composition, but to date there is only one case which has been accessible to this kind of analysis: the gravitationally lensed galaxy MS 1512-cB58 at $z = 2.7276$ (see Figure 4). The relative underabundance of elements produced by intermediate and low mass stars, compared to the products of Type II supernovae, is highly suggestive of a rapid timescale for the build-up of metals, of the order of a few hundred million years, consistent with the very high star formation rates—typically tens of solar masses per year—exhibited by these UV-bright galaxies.

3.2 Damped Lyman α Systems

Abundance measurements are now also available for over one hundred damped Ly α systems. Zinc has played an important role in this context because, unlike most other Fe-peak elements, it is normally undepleted onto dust and the resonance doublet of its major ionisation stage in H I regions, Zn II $\lambda\lambda 2026, 2062$, is well placed for observations from the ground over a wide range of redshifts (Pettini, Boksenberg, & Hunstead 1990). The latest published compilation of $[Zn/H]$ determinations in DLAs by Kulkarni et al. (2005) includes 87 measurements or upper limits, mostly obtained from echelle spectroscopy with large telescopes (see Figure 5). It is clear from these data that absorption-selected galaxies give quite a different picture of chemical enrichment at high redshift from that obtained when considering the bright galaxies detected directly via their emission. First, DLAs are mostly metal poor. Adding up all the Zn and H separately, we obtain the column density-weighted mean metallicity $[\langle Zn/H \rangle] = -1.2$ (or $Z \simeq 1/15Z_{\odot}$) at $1.8 < z < 3.5$. Second, there is a wide dispersion in metallicity among DLA galaxies at the same epoch, with individual values of the Zn abundance spanning two orders of magnitude, from solar to less than 1/100 of solar.

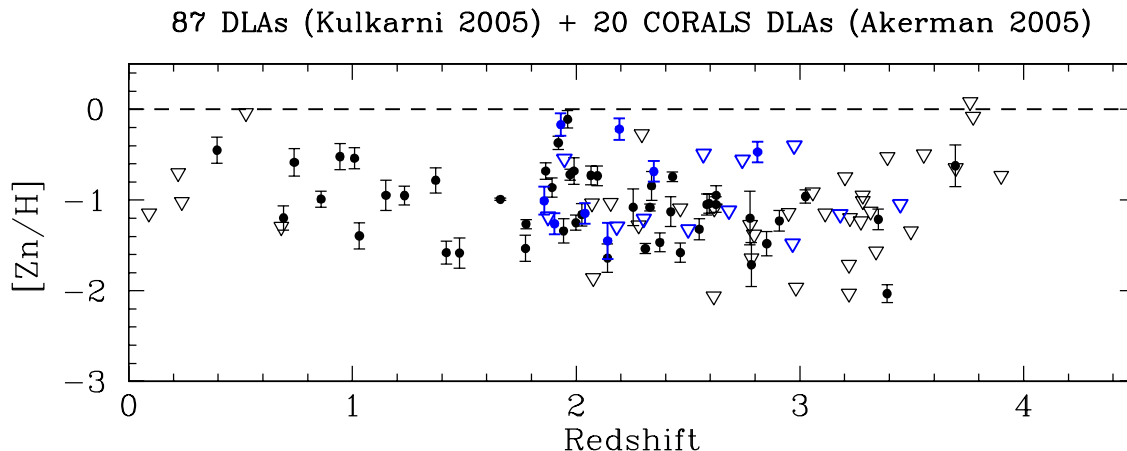


Figure 5: Zn abundances in DLAs, from the compilation by Kulkarni et al. 2005 (black), which brings together the results of several surveys for DLAs in optically selected QSO samples, and from the recent survey of CORALS (radio-selected) QSOs by Akerman et al. 2005 (blue). Triangles denote upper limits in DLAs whose Zn II $\lambda\lambda 2026, 2062$ lines remain undetected.

3.2.1 Dust-induced bias? The consistently low metallicity of DLAs at all redshifts has been a cause of concern for models which use them to track the global evolution of baryons through the cosmic ages (e.g. Pei & Fall 1995; Kulkarni & Fall 2002; Nagamine, Springel, & Hernquist 2004; Wolfe et al. 2005). The biasing effects of dust have been invoked by many as a possible explanation of this apparent puzzle. DLAs are generally culled from QSO surveys which are magnitude limited and the brighter ones tend to be selected for subsequent

spectroscopic follow-up for practical reasons of S/N and resolution. It thus seems plausible that the most metal-rich members of a distribution of metallicities may be preferentially missing from current samples, if the background QSOs against which they would be seen are sufficiently dimmed by dust in the very absorbers being sought.

Despite the appeal of its simplicity, the possibility that dust may be significantly distorting our view of high redshift QSOs and their intervening absorbers has turned out to be unsupported by the available data: DLAs with the required characteristics appear to be genuinely rare since they have not been found even in surveys which use radio-selected QSOs as background sources, where dust bias is presumably not an issue (Ellison et al. 2001). As can be appreciated from Figure 5, the Zn abundance of DLAs in the (radio-selected) CORALS sample is not significantly different than that of the bulk of known DLAs drawn from magnitude limited optical samples of QSOs. Akerman et al. (2005) deduced a column density-weighted metallicity $[\langle \text{Zn}/\text{H} \rangle] = -0.87 \pm 0.13$ for CORALS DLAs, only marginally higher than the corresponding value $[\langle \text{Zn}/\text{H} \rangle] = -1.17 \pm 0.07$ determined from optical surveys over the same redshift interval, and concluded that the two sets of data are consistent with being drawn from the same parent distribution at the 90% confidence level.

The recent detection of dust reddening associated with Ca II-selected DLAs at $z \sim 1$ in SDSS QSOs (Wild, Hewett, & Pettini 2006) confirms that the level of extinction remains generally low until these later epochs, since even this subset of absorbers, with rather extreme properties compared to typical DLAs, introduces only a modest $\langle E(B - V) \rangle < 0.1$ mag.

3.2.2 Systematic offset between absorption- and emission-measured abundances? The apparent ‘disconnect’ in metallicity between star-forming galaxies and DLAs at the same cosmic epochs has led some to question whether there might be systematic offsets between abundances measured in H II and H I regions—a possibility apparently admitted by recent *Far-Ultraviolet Spectroscopic Explorer* (FUSE) observations of low metallicity dwarf galaxies, although the interpretation of the FUSE data is far from straightforward (Cannon et al. 2005). Such offsets, if present, may be due to: (a) systematic errors in the abundance determinations; (b) abundance gradients between the inner, high surface density, star-forming regions of a galaxy and its outer regions which present the larger cross-section for absorption against a background source; or (c) in a more general sense, the existence of extended envelopes of unprocessed gas on the outskirts of galaxies.

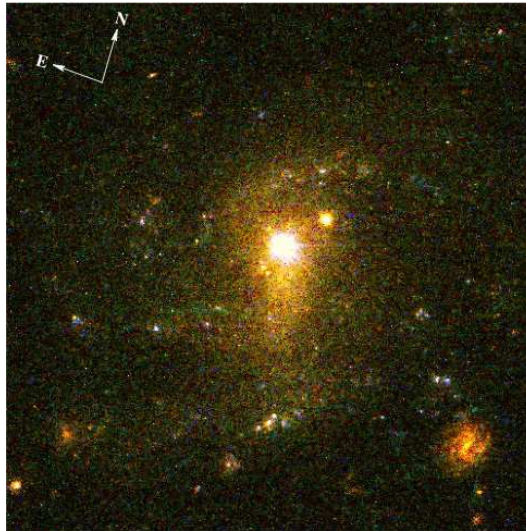


Figure 6: *Hubble Space Telescope* (WFPC2) image of the nearby ($d = 43.3 h_{70}^{-2}$ Mpc) dwarf ($M_B = -16.8$) galaxy SBS 1543+593 (reproduced from Schulte-Ladbeck et al. 2004). The portion of the WFPC2 image shown here is 50×50 arcsec, corresponding to 10.4×10.4 kpc at the distance of the galaxy. The bright source near the centre of the galaxy is not its nucleus, but a background ($z_{\text{em}} = 0.807$) QSO in whose spectrum the ISM of the dwarf galaxy produces a DLA with $\log N(\text{H I}) = 20.42$ (where N is the column density in units of cm^{-2}). The metallicity of the DLA is the same as that of the brightest H II region in the galaxy, located 3.3 kpc directly below its centre in this image.

The ‘cleanest’ test of these hypotheses was recently performed by Bowen et al. (2005) who found the abundance of S in the neutral ISM of the dwarf galaxy SBS 1543+593 to be the same as that of O in an H II region 3.3 kpc away (see Figure 6). This comparison is particularly meaningful because S and O are both alpha-capture elements (i.e. they share similar nucleosynthetic histories) and corrections for dust depletion are normally small for both elements. This reassuring consistency check excludes options (a) and (c) above—at least in the case of this galaxy. However, it provides no information on the importance of abundance gradients, particularly at high redshifts, because today’s dwarf galaxies do not exhibit significant radial gradients in their metallicity.

3.2.3 *Clues from element ratios.* As well as exhibiting widely different degrees of metal enrichment, DLAs also appear to be quite a ‘mixed bag’ in their detailed chemical composition. For example, no clear pattern emerges from consideration of the relative proportions of alpha-capture to Fe-peak elements. In DLAs the $[\alpha/\text{Fe}]$ ratio is most conveniently measured via $[\text{S}/\text{Zn}]$, two elements which show little affinity for dust and whose first ions (the dominant ion stages in H I regions) have absorption lines which generally are not heavily saturated in DLAs. On the other hand, the fact that these transitions are separated by nearly 800 Å in the rest frame ultraviolet restricts the redshift range over which they can both be measured in the same absorption system. For this reason, the current sample of $[\text{S}/\text{Zn}]$ measurements in DLAs is still relatively small (see Figure 7). Nevertheless, the available data indicate that while some DLAs may conform to the Milky Way pattern of enhanced $[\alpha/\text{Fe}]$ ratios at metallicities $[\text{Fe}/\text{H}] \lesssim -1$, many of them evidently do not, exhibiting solar or even sub-solar values of $[\text{S}/\text{Zn}]$. In the context of current galactic chemical evolution models, such low ratios are interpreted as evidence for generally low, or intermittent, rates of star formation (e.g. Pagel & Tautvaišienė 1995; Matteucci & Recchi 2001).

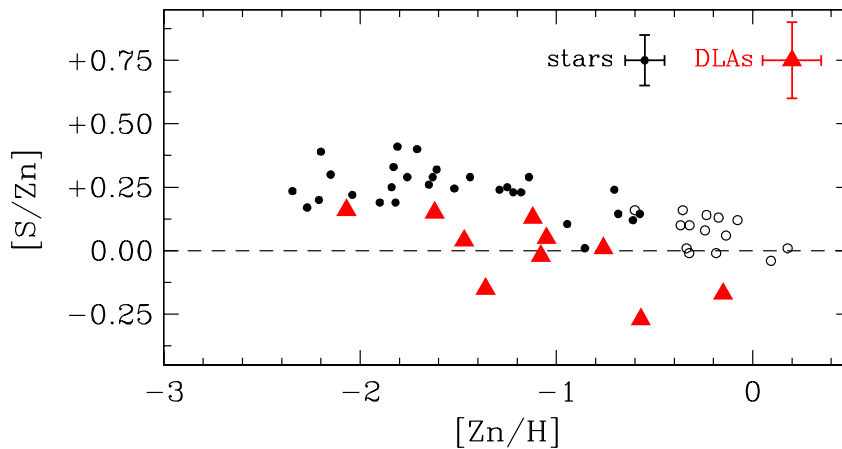


Figure 7: Relative abundances of S (an α -capture element) and Zn (an Fe-peak element) in Galactic disk (open circles) and halo (filled circles) stars and in DLAs (red triangles). Typical errors in the abundance determinations are shown in the top right-hand corner. The existing, small, sample of damped systems in which both S and Zn have been measured does not show clear evidence of the α -element enhancement at low metallicities typical of Milky Way stars, but a wider spread of $[\alpha/\text{Fe}]$ ratios—a further demonstration of the heterogeneous nature of DLA galaxies. (Figure reproduced from Nissen et al. 2004).

4 The Link to Today’s Galaxies

4.1 Star-Forming Galaxies at $z \gtrsim 2$: Ellipticals and Bulges in the Making

The near-solar metallicities measured in star-forming galaxies at $z = 2 - 3$ —whether selected at optical, IR, or sub-mm wavelengths—are just one strand of a multi-faceted picture which has emerged in the last few years linking these objects to the bulge component of today’s galaxy population, as originally proposed by Steidel et al. (1996). Their emission properties at X-ray (Reddy & Steidel 2004) and mid-IR (Reddy et al. 2006) wavelengths indicate star formation rates $\text{SFR} \gtrsim 10 M_{\odot} \text{ yr}^{-1}$ (for galaxies brighter than $\mathcal{R} = 25.5$) and an average bolometric luminosity $\langle L_{\text{bol}} \rangle \simeq 3 \times 10^{11} L_{\odot}$. Their spectral energy distributions, which have now been determined from the rest-frame UV to the near-IR thanks to the highly successful *Spitzer* Space Telescope, indicate that these high star formation rates typically persist for several hundred million years, leading to the rapid assembly of stellar masses $M_{*} \gtrsim 10^{10} M_{\odot}$ (see Figure 8). In models of galaxy formation which couple cosmological simulations of dark matter haloes with the physics and dynamics of the baryons (e.g. Blaizot et al. 2004; Mori & Umemura 2006) objects exhibiting these properties at $z = 2 - 3$ naturally evolve to become today’s massive and metal-rich elliptical galaxies.

The closest, and best studied, spiral bulge is that of the Milky Way where the properties of individual stars can be determined. Most models which have been proposed to explain the distributions of stellar ages, metallicities, and element ratios (e.g. Ferreras, Wyse, & Silk 2003) share the same basic ingredients: (a) an early epoch of formation, at $z \sim 5$; (b) short infall timescales, $\tau < 0.5$ Gyr, leading to a rapid enrichment to near-solar metallicity and enhanced $[\alpha/\text{Fe}]$ ratios; and (c) significant outflow of gas and metals accompanying the collapse and star formation process, resulting in a final stellar mass $M_{*} \sim 10^{10} M_{\odot}$. These characteristics are very much in line with those determined for a typical UV-selected (‘BX’) galaxy at $z \sim 2$, although galaxies

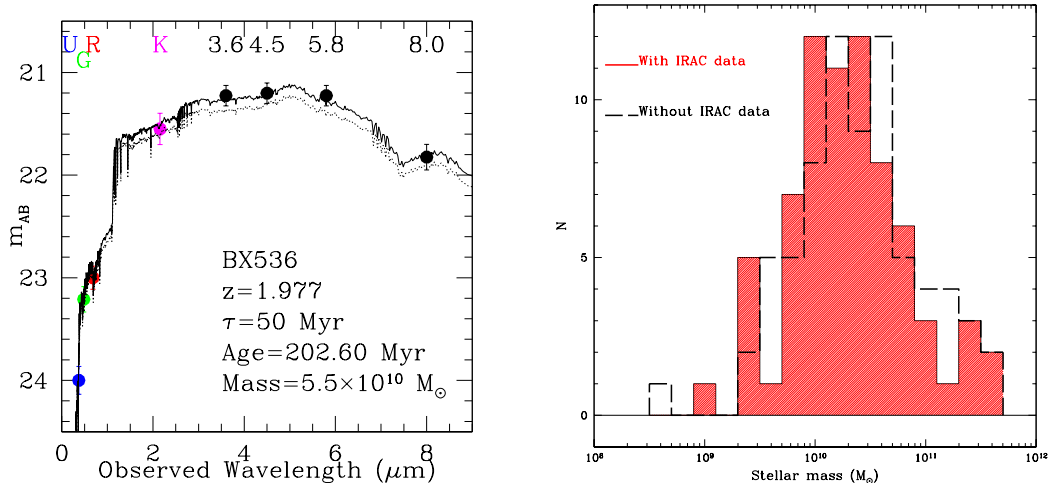


Figure 8: *Left*: Model spectral energy distributions (continuous lines) which best fit the rest-frame UV to near-IR photometry of Q1700-BX536, a typical star-forming galaxy at $z \simeq 2$. The bottom curve shows the result of fitting to the *UGRK* magnitudes only (that is, it excludes the *Spitzer* IRAC data points). The values of the parameters which characterise the best-fitting model—e-folding time scale of declining star formation, age, and assembled stellar mass—are given in the bottom right-hand corner. *Right*: Histograms of assembled stellar masses for the 72 BX galaxies with spectroscopic redshifts in the field of the $z_{\text{em}} = 2.72$ QSO HS1700+643. The median stellar mass of $z \simeq 2$ galaxies brighter than $\mathcal{R} \simeq 25.5$ is $2 \times 10^{10} M_{\odot}$. Both figures have been reproduced from Shapley et al. (2005).

which *end up* with an assembled stellar mass of only $M_* \sim 10^{10} M_{\odot}$ are probably near, or below, the faint end of the observed luminosity distribution.

Perhaps the most compelling evidence linking the UV- and IR-bright galaxies at $z = 2 - 3$ with today’s elliptical galaxies is provided by their clustering properties (see Figure 9). As shown by Adelberger et al. (2005b), the high redshift populations are highly clustered, with correlation lengths $r_0 = 4.0 - 4.5 h^{-1} \text{Mpc}$. In cosmological simulations, dark matter halos with these values of r_0 have masses $M_{\text{DM}} = 10^{11.2} - 10^{12.3} M_{\odot}$; evolved forward in time their clustering and number density are a much better match to those of elliptical galaxies than spirals. There are also indications that in the largest galaxy overdensities at $z \simeq 2$ star formation started earlier than in the field, as expected within the general framework of hierarchical clustering theories of the evolution of structure. As a consequence, galaxies within these overdensities tend to have higher stellar masses and metallicities than the mean values for the population as a whole (Steidel et al. 2005).

4.2 DLAs: Early Stages in the Formation of Spiral Galaxies?

While an evolutionary link between star-forming galaxies at $z = 2 - 3$ and the spheroidal component of the galaxy population today is strongly suggested by the available evidence, an analogous connection for DLAs is still a matter for debate. The working hypothesis that in DLAs we see the progenitors of today’s disk galaxies like the Milky Way (Wolfe et al. 1986), while consistent with the kinematics of the associated metal absorption lines (Wolfe et al. 2005), runs into some difficulties when confronted with the metallicity data (see Figure 10). Current models (e.g. Naab & Ostriker 2006) envisage the Milky Way disk to have been significantly smaller at $z = 2 - 3$ (that is, disk growth is from ‘inside out’), and this would indeed explain why direct detection of the stellar light from DLA host galaxies at $z > 1$ has proved so elusive (Wolfe et al. 2005 and references therein). However, even in the early stages of its evolution, the disk was already more metal rich than most DLAs, with $Z \simeq 1/3 Z_{\odot}$; the flat age-metallicity relation of disk stars implies that the epoch when the metallicity of the Milky Way was below this value was brief (e.g. Akerman et al. 2004). Consequently, there is little overlap between the metallicity distributions of the DLAs on the one hand, and of stars in the thin and thick disks of the Galaxy on the other (Figure 10).

The low metallicities of most DLAs may be reconciled with the proposed origin in spiral galaxies if, during their assembly, disk galaxies were surrounded by extended envelopes (a halo, or a thick disk) of neutral gas which was metal-poor, or had a steep metallicity gradient. Such a scenario has been proposed by Wolfe et al. (2003) and may be the explanation for the very extended stellar disk structures recently found in galaxies such as M31 (Ibata et al. 2005). Simulations of the growth of disk galaxies through mergers of gas-rich subunits (e.g. Navarro 2004; Governato et al. 2005) can reproduce many of the characteristics of the Local Group of galaxies—it will be of considerable interest to examine in more detail the properties of the gaseous components of such mergers during this early build-up epoch with an eye to their possible interpretation as DLAs.

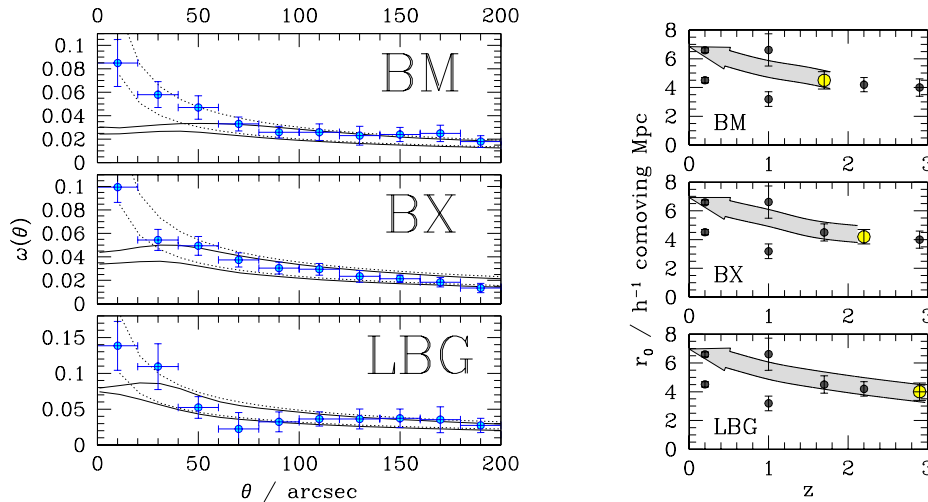


Figure 9: *Left*: Angular clustering on the sky of ‘BM’ ($\langle z \rangle = 1.7$), ‘BX’ ($\langle z \rangle = 2.2$), and Lyman break ($\langle z \rangle = 3.0$) galaxies (data points) and of dark matter halos from cosmological simulations (continuous lines). The simulations match the observations for halo masses in the range $M_{\text{DM}} = 10^{11.2} - 10^{12.3} M_{\odot}$. *Right*: The arrows show the evolution seen in the simulations for halos within the mass ranges which match the observed galaxy clustering. The BM, BX, and LBG samples seem to trace the same objects—or, more precisely, the same halo mass range—through different evolutionary stages. When evolved to intermediate and low redshifts, their clustering matches that of elliptical galaxies in the DEEP and 2dF surveys (the two upper data points at $z = 1$ and 0.2), rather than that of galaxies which are still forming stars at these later epochs (lower data points). Both figures have been reproduced from Adelberger et al. (2005b).

One of the most significant advances towards answering the long-standing question of which galaxies give rise to damped Ly α systems is the recent work by Zwaan et al. (2005) who tackled the problem ‘from the other end’, as it were, by considering the H I properties of local galaxies. Based on 21 cm column density maps of nearly 400 galaxies, obtained as part of the Westerbork H I survey of spiral and irregular galaxies (WHISP) and covering all Hubble types and a wide range in luminosity, the analysis by Zwaan et al. has shown that the distribution of luminosities of the galaxies producing DLAs is nearly flat from $M_B = -21$ to $M_B = -15$. Thus, at $z = 0$, galaxies spanning over two orders of magnitude in luminosity evidently make roughly comparable contributions to the overall cross-section on the sky for DLA absorption. If this is also the case at high z , the heterogeneous nature of DLA absorbers provides a plausible explanation for the wide dispersion in their physical properties, including metallicity.

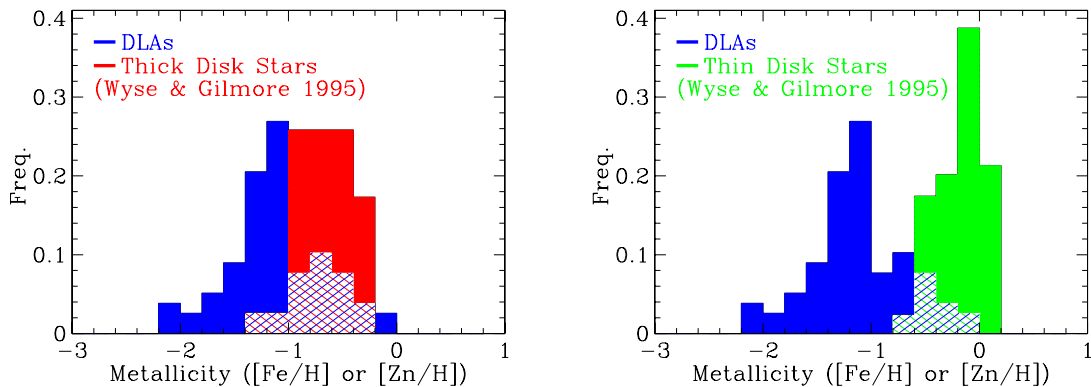


Figure 10: Metallicity distributions of DLAs and Milky Way thick (left panel) and thin (right panel) disk stars from the work by Akerman et al. (2005). The metallicity is measured from Zn in DLAs and Fe in Galactic stars. Approximately one half of the DLA measurements of $[\text{Zn}/\text{H}]$ are upper limits; they have been included in the histograms as if they were detections.

5 Conclusions

5.1 A Snapshot of Metallicity at $z = 2.5$

The recent results summarised in this review have fleshed out further the overall picture of element abundances at high redshift which has been gradually coming into focus over the last few years. When we plot the metallicities measured in different environments against the typical physical scale of the structures to which they refer, as in Figure 11, we find a clear trend of decreasing metal abundance with increasing scale. Another way to interpret the trend is to view the x -axis of Figure 11 as a scale of decreasing overdensity relative to the cosmic mean. Thus, at $z = 2.5$, which corresponds to 2.5 Gyr after the Big Bang in today’s consensus cosmology, the gas in the inner 10–100 pc of the highest overdensities, where supermassive black holes reside, has already been enriched to supersolar proportions (e.g. Hamann et al. 2002). Galaxies which are undergoing active star formation, at rates comparable to those of today’s Luminous Infrared Galaxies, exhibit near-solar metallicities on kpc scales. DLAs probably sample more diffuse gas, possibly on the outskirts of galaxies in the process of formation and, in any case, appear to be quite a heterogeneous population exhibiting more than two orders of magnitude of dispersion in their degree of metal enrichment. Finally, the Lyman α forest which traces large scale structures of moderate overdensity relative to the cosmic mean (and which could not be included in this review due to lack of space) contains only trace amounts of metals (whose origin is still the matter of some debate—see Adelberger 2005a and Songaila 2006).

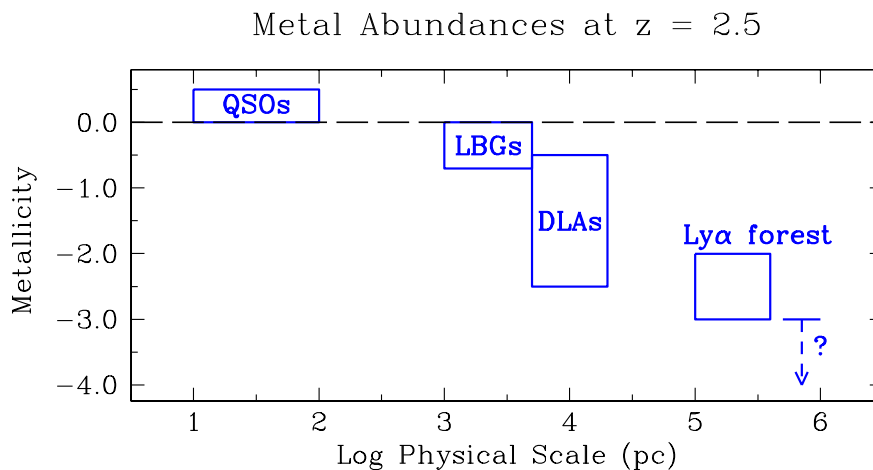


Figure 11: Snapshot of the metallicity of different components of the high redshift universe. The logarithm of the metallicity is plotted relative to solar (indicated by the long-dash line at 0.0) against the typical linear scale of the structures to which it refers. The term “Lyman break galaxies” (LBGs) is used as a shorthand here to refer to a more general class of actively star-forming galaxies.

Evidently, it is the depth of the potential well within which the baryons find themselves that drives the pace at which gas is processed through stellar nucleosynthesis. Thus, at any one epoch, there can be a range of three-to-four orders of magnitude in the degree of metal enrichment which one would measure, depending on environment.

5.2 Metallicity Evolution

Conversely, metallicity depends weakly on cosmic time—the age-metallicity relation of the universe as a whole appears to be shallow, just as is the case for the stellar disk of the Milky Way. This is the conclusion reached by the first attempts to assess the degree of evolution with look-back time of relationships which are well established in the present-day universe, such as the luminosity-metallicity and mass-metallicity relations. The obstacles faced by such endeavours are considerable. One is the obvious requirement that we should employ measures of metallicity which can be applied self-consistently over a wide range of redshifts. This is not straightforward to implement, as explained in the preceding sections, but in principle should be a tractable problem given sufficient telescope time and attention to detail. Far less clear is how to isolate some meaningful property which we can hold constant with redshift and against which metallicity is to be measured—in an evolving universe how can we be sure that we are comparing the same kinds of objects at different epochs?

One of the first attempts in this direction is that by Kewley & Kobulnicky (2005) who deduced a slope of -0.15 dex per unit redshift in the oxygen abundance of luminous galaxies, brighter than $M_B = -20.5$ or approximately L^* (see also Maier, Lilly & Carollo 2005). A similarly shallow slope is exhibited by the redshift

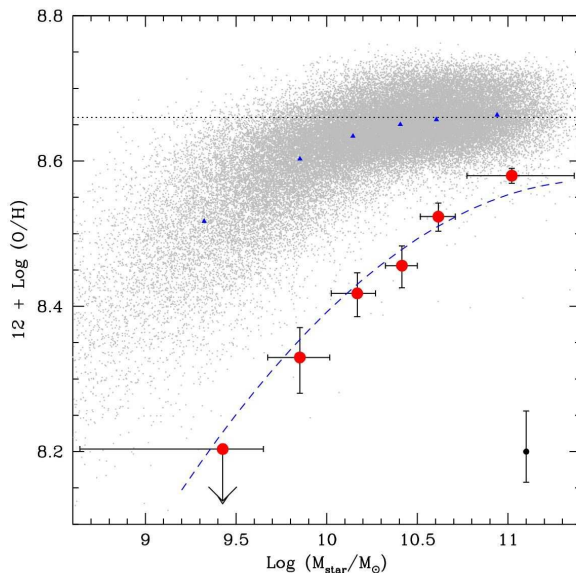


Figure 12: Stellar mass-metallicity relation for star-forming galaxies at $z \sim 2$ (large red circles with error bars) and in the nearby ($z \sim 0.1$) universe from the SDSS survey (small grey points). The blue triangles show the mean metallicity of the SDSS galaxies in the same mass bins as the $z = 2$ galaxies. The vertical error bar in the bottom right-hand corner indicates the uncertainty in the calibration of the $N2$ index used to deduce the oxygen abundance of both sets of galaxies. Since the $N2$ index saturates near solar metallicity (indicated by the horizontal dotted line), the offset between the present-day and high-redshift relations is best derived by consideration of the lower metallicity bins. At a given assembled stellar mass, galaxies at $z = 2$ appear to be about a factor of two lower in metallicity than today. (Figure reproduced from Erb et al. 2006a).

evolution of the metallicity of DLAs (Kulkarni et al. 2005). In other words, from $z = 3$ to 0 the average (O/H) increased by a mere factor of three: this is modest evolution indeed, compared with the orders-of-magnitude dispersion at a given epoch seen in Figure 11. The difficulty lies in the interpretation of M_B , given that we are most likely dealing with objects of very different mass-to-light ratios at different redshifts, as shown by Shapley et al. (2005).

In this respect mass is probably a more physically meaningful quantity than light. While we cannot determine directly the masses of the dark matter halos in which *individual* galaxies reside (the resolution and sensitivity required to, for example, trace 21 cm rotation curves at high redshift are still years away), we do have estimates of the assembled stellar mass—the integral of the past star formation rate over the age of the galaxies—as discussed in section 4.1. When compared with the present-day mass-metallicity relation (see Figure 12), we find again only a modest degree of evolution: galaxies of a given stellar mass are on average about a factor of two lower in metallicity at $z \simeq 2$ than today, consistent with the shallow metallicity-redshift gradient deduced by Kewley & Kobulnicky (2005) and by Kulkarni et al. (2005). The more significant shift in Figure 12 is along the x -axis, as pointed out by Savaglio et al. (2005): galaxies which had attained a given metallicity were one order of magnitude more massive at $z \simeq 2$.¹ This ‘evolution’ is in the sense of the conclusions we drew from Figure 11, reinforcing the idea that the cycling of gas through stars proceeds at a pace determined primarily by the overdensity of the objects which have collapsed to form bound structures.

5.3 A Revised Census of Metals at $z = 2.5$

The recent advances in determining the physical properties of galaxies at high redshift summarised in this review warrant revisiting the ‘Missing Metals’ problem discussed by Pagel (2002) and Pettini (2004), and more recently reconsidered by Bouché, Lehnert, & Péroux (2005). Briefly, the (unobscured) ultraviolet luminosity of galaxies is also a measure of the metal production rate, since the same massive stars produce the UV photons and the metals which are promptly released into the ISM. One can thus integrate the comoving star formation rate deduced from galaxy surveys and, with appropriate conversion factors, obtain an estimate of the comoving density of metals which have accumulated in the universe by a given redshift. A simple consistency check is to compare this quantity with the metallicity of different components of the high redshift universe and thereby

¹This statement is correct only if the relationship between metallicity and gas fraction does not change significantly among galaxies of different masses and at different redshifts. Clearly this is an oversimplification, only applicable to a ‘closed box’ model of galactic chemical evolution with a universal IMF. Nevertheless, if variations in the effective yield—which links metallicity and gas fraction—are not extreme, then the above conclusion is valid to a first approximation.

obtain an indication of how (in)complete our census of metals at high z is. Initial indications (Pagel 2002; Pettini 2004) pointed to a significant deficit in the metals accounted for by LBGs, DLAs and the Lyman α forest, which we are now ready to reexamine with improved data.

I begin by recalculating the total metal production up to $z = 2.5$. Recent studies of the X-ray (Reddy & Steidel 2004) and mid-IR (Reddy et al. 2006) luminosities of (rest-frame) UV-selected galaxies at $z = 2 - 3$, making use of the very deep imaging at many wavelengths of the GOODS-N field, have placed on more secure footing estimates of the extinction correction applicable to UV-deduced star formation rates. The typical correction factor of 4.5-5 obtained by Reddy & Steidel (2004) is in excellent agreement with the value of 4.7 adopted by Steidel et al. (1999) from consideration of the observed UV spectral slope of Lyman break galaxies. Furthermore, the GOODS-N field also allowed different photometric selections of high z galaxies to be compared quantitatively. Reddy et al. (2005) considered the contribution of optical, near-IR, and sub-mm selected galaxies to the star formation rate density at $z \sim 2$, taking into account sample overlap, and concluded that optically (rest-frame UV) selected galaxies brighter than $\mathcal{R} = 25.5$ (the limit of the surveys by Steidel and collaborators) account for $\sim 70\%$ of the total. Star formation and metal ejection rates are related by $\dot{\rho}_* = 64 \dot{\rho}_Z$ according to the recent estimate by Conti et al. (2003); this conversion factor is a reduction by a factor of 1.5 in the metal production rate compared to the original estimate by Madau et al. (1996). With these updates, and converting the estimates of the star formation rate density by Steidel et al. (1999) to today's consensus cosmology ($\Omega_M = 0.3$, $\Omega_\Lambda = 0.7$, $H_0 = 70 \text{ km s}^{-1} \text{ Mpc}^{-1}$), we obtain:

$$\int_{11 \text{ Gyr}}^{13 \text{ Gyr}} \dot{\rho}_Z dt \simeq 3.4 \times 10^6 M_\odot \text{ Mpc}^{-3}. \quad (1)$$

This value is obtained under the assumption that star formation in the universe began at $z = 10$ (0.46 Gyr after the Big Bang) at levels similar to those measured at $z = 4 - 5$. An increasing star formation rate density from $z = 10$ to 4, as proposed by Bouwens et al. (2005—see also these proceedings) and Bunker et al. (2005), would reduce the above estimate by about one quarter.

A comoving density of metals of $3.4 \times 10^6 M_\odot \text{ Mpc}^{-3}$ corresponds to

$$\Omega_Z \simeq 0.045 \times (\Omega_{\text{baryons}} \times 0.0126) \quad (2)$$

where $\Omega_{\text{baryons}} = 0.044$ (Pettini 2005) of $\rho_{\text{crit}} = 1.35 \times 10^{11} M_\odot \text{ Mpc}^{-3}$ (both for $h_{70} = 1$) and 0.0126 is the mass fraction of elements heavier than helium for solar metallicity (Asplund et al. 2004). The value of Ω_Z obtained here is not very different from that calculated by Pettini (2004) because the various updates to the measurements on which it is based largely compensate each other. It implies that the star formation activity we believe to have taken place between the Big Bang and $z = 2.5$ (2.5 Gyr later) was sufficient to enrich the universe as whole to a metallicity of 4–5% of solar.

TABLE 1
CENSUS OF METALS AT $z = 2.5^a$

Component	Ω^b	Z^c	Ω_Z^d
Observed:			
Ly α Forest	4.1×10^{-2}	6.3×10^{-3}	5.9×10^{-3}
DLAs	8.5×10^{-4}	1.35×10^{-1}	2.6×10^{-3}
UV-selected Galaxies	6.4×10^{-4}	6×10^{-1}	8.8×10^{-3}
Total Observed:			1.7×10^{-2}
Predicted:			4.5×10^{-2}

^aAll entries are for $H_0 = 70 \text{ km s}^{-1} \text{ Mpc}^{-1}$; $\Omega_M = 0.3$, $\Omega_\Lambda = 0.7$.

^bIn units of the closure density $\rho_{\text{crit}} = 1.35 \times 10^{11} h_{70}^2 M_\odot \text{ Mpc}^{-3}$.

^cIn units of solar metallicity (0.0126 by mass).

^dIn units of $\Omega_{Z_\odot} = \Omega_{\text{baryons}} \times Z_\odot = 5.5 \times 10^{-4}$.

Table 1 assesses the contributions of the Lyman α forest, DLAs and UV-selected galaxies to the total metal budget. For the Lyman α forest I quote the results of the careful study by Simcoe, Sargent, & Rauch (2004), based on associated C IV and O VI absorption in QSO spectra of very high S/N. For DLAs, $\Omega_{\text{DLA}} = 8.5 \times 10^{-4}$ is indicated by the improved statistics of the SDSS (Prochaska, Herbert-Fort, & Wolfe 2005), and $Z_{\text{DLA}} = 2/15 Z_\odot$

is the value implied by the column density-weighted metallicity $[\langle Z_{\text{N}}/H \rangle] = -0.87 \pm 0.13$ of Akerman et al. 2005 (no correction has been applied for a possible underabundance of the Fe-peak elements relative to elements which are released promptly into the ISM because such an effect is generally not seen in DLAs—see Figure 7). When added together, QSO absorbers (the Lyman α forest and DLAs) make up less than 20% of the required $\Omega_Z \simeq 0.045$ (last column of Table 1); interestingly, these recent estimates indicate that there are approximately twice as many metals in the forest as in DLAs. Lyman limit systems (sometime referred as sub-DLAs) have not been included in our accounting, because their comoving mass density and metallicity have not yet been established with certainty. If the gas in sub-DLAs is mostly ionised, their contribution to the metal budget could be significant (P eroux et al. 2005). We could also be missing metals in the Lyman α forest, if they are in a hot phase which does not give rise to detectable C IV and O VI absorption lines.

Let us now turn to UV-selected galaxies. Adelberger & Steidel (2000) showed that the luminosity function of LBGs at $z = 3$ is well fitted by a Schechter function with faint end slope $\alpha = -1.6$, characteristic magnitude $m_*(\mathcal{R}) = 24.54$, and normalisation $\Phi_* = 1.5 \times 10^{-3} h_{70}^3 \text{Mpc}^{-3}$. These parameters do not appear to change from $z \simeq 4$ (Steidel et al. 1999) to $z \simeq 2$ (Reddy et al. in preparation), apart from the scaling of $m_*(\mathcal{R})$ in accordance to the luminosity distance and k -corrections applicable to the different redshifts. Thus, the comoving density of UV-selected galaxies brighter than $\mathcal{R} = 25.5$ ($\approx 1/4 m_*$) at $z = 2.2$ (the median redshift of the BX sample to which the metallicity measurements discussed in §3.1 refer) is $2.4 \times 10^{-3} \text{Mpc}^{-3}$.

The work of Erb et al. (2006a) has provided estimates of the baryonic mass (stars+gas) and oxygen abundance for a sample of nearly one hundred such galaxies: masses range between $\log(M/M_{\odot}) = 11.1$ and 10.3, and metallicities between approximately solar to less than 1/3 solar. A proper accounting would integrate the mass-weighted metallicity of these galaxies; however, such an approach would require a knowledge of the mass function of BX galaxies, which has yet to be determined. Given the relatively small range of baryonic masses and metallicities indicated by the analysis of Erb et al. (2006a), we may be justified in adopting the median values of the sample as a first approximation. Thus, combining the median baryonic mass of BX galaxies $\langle M_{\text{BX}} \rangle = 3.6 \times 10^{10} M_{\odot}$ with their comoving volume density given above, we obtain a total baryonic mass density $\Omega_{\text{BX}} = 6.4 \times 10^{-4}$. With a typical metallicity $Z_{\text{BX}} \simeq 0.6 Z_{\odot}$, the metal content of UV-selected galaxies amounts to $\Omega_Z = 8.8 \times 10^{-3}$.

In reality, this is likely to be an underestimate because the data of Erb et al. show a correlation between mass and metallicity at the high mass end (see Figure 8 of Erb et al. 2006a), so that the more massive galaxies contain proportionally more metals. Furthermore, we have not included in our accounting galaxies which are missed by the UV photometric selection technique but included in near-IR and sub-mm surveys. To date the masses and metallicities of these objects are less well determined than those of UV-selected galaxies. These different samples of high redshift galaxies do overlap, as shown by Reddy et al. (2005) who concluded that the galaxies missed by the UV selection account for $\sim 30\%$ of the star formation rate density at $z \simeq 2$. However, such galaxies may contribute a larger fraction of the metals, if they include a high proportion of evolved objects which have attained a high metallicity (e.g. Dunne, Eales, & Edmunds 2003).

If we add up the contributions of the Lyman α forest, DLAs and UV-selected galaxies (last column of Table 1), we can account for $\sim 40\%$ of the metal production from the Big Bang to $z = 2.5$. With the addition of metals in sub-DLAs, in the most massive UV-selected galaxies, and in galaxies missed by the BX photometric criteria—all unaccounted for in the estimates above—we may well have solved the ‘Missing Metals’ problem. Perhaps this is an indication that our knowledge of the high redshift galaxy population has indeed improved in the last few years.

Acknowledgements. It is a pleasure to acknowledge my collaborators in the various projects described in this review, particularly Kurt Adelberger, Chris Akerman, David Bowen, Sara Ellison, Dawn Erb, Naveen Reddy, Sam Rix, Alice Shapley and Chuck Steidel. I am indebted to Bernard Pagel for numerous inspiring conversations over the years, and I am grateful to him, Miroslava Dessauges-Zavadsky, Varsha Kulkarni, Claus Leitherer, and Christy Tremonti for valuable comments on this paper. Finally, I thank the conference organisers for financial support which helped me take part in this stimulating meeting.

References

- [1] Adelberger, K. L. 2005a, in *Probing Galaxies through Quasar Absorption Lines*, IAU Colloquium 199, P. R. Williams, C. Shu, & B. M enard eds. (Cambridge: Cambridge University Press), 341
- [2] Adelberger, K. L. & Steidel, C. C. 2000, *ApJ*, 544, 218
- [3] Adelberger, K. L., Steidel, C. C., Pettini, M., Shapley, A. E., Reddy, N. A., & Erb, D. K. 2005b, *ApJ*, 619, 697
- [4] Adelberger, K. L., Steidel, C. C., Shapley, A. E., Hunt, M. P., Erb, D. K., Reddy, N. A., & Pettini, M. 2004, *ApJ*, 607, 226
- [5] Akerman, C. J., Carigi, L., Pettini, M., Nissen, P. E. & Asplund, M. 2004, *A&A*, 414, 931

- [6] Akerman, C. J., Ellison, S. L., Pettini, M., & Steidel, C. C. 2005, *A&A*, 440, 499
- [7] Asplund, M., Grevesse, N., Sauval, A. J., Allende Prieto, C., & Kiselman, D. 2004, *A&A*, 417, 751
- [8] Blaizot, J., Guiderdoni, B., Devriendt, J. E. G., Bouchet, F. R., Hatton, S. J., & Stoehr, F. 2004, *MNRAS*, 352, 571
- [9] Bouché, N., Lehnert, M. D., & Péroux, C. 2005, *MNRAS*, 364, 319
- [10] Bouwens, R. J., Illingworth, G. D., Thompson, R. I., & Franx, M. 2005, *ApJ*, 624, L5
- [11] Bowen, D. V., Jenkins, E. B., Pettini, M., & Tripp, T. M. 2005, *ApJ*, 635, 880
- [12] Bunker, A., Stanway, E., Ellis, R., McMahon, R., Eyles, L., & Lacy, M. 2005, in *First Light and Reionization*, E. Barton & A. Cooray eds., *New Astronomy Reviews*, in press (astro-ph/0508271)
- [13] Cannon, J. M., Skillman, E. D., Sembach, K. R., & Bomans, D. J. 2005, *ApJ*, 618, 247
- [14] Conti et al. 2003, *AJ*, 126, 2330
- [15] de Mello, D. F., Daddi, E., Renzini, A., Cimatti, A., di Serego Alighieri, S., Pozzetti, L., & Zamorani, G. 2004, *ApJ*, 608, L29
- [16] Dunne, L., Eales, S. A., & Edmunds, M. G. 2003, *MNRAS*, 341, 589
- [17] Ellison, S. L., Yan, L., Hook, I. M., Pettini, M., Wall, J. V., & Shaver, P. 2001, *A&A*, 379, 292
- [18] Erb, D. K., Shapley, A. E., Pettini, M., Steidel, C. C., Reddy, N. A., & Adelberger, K. L. 2006a, *ApJ*, in press (astro-ph/0602473)
- [19] Erb, D. K., Steidel, C. C., Shapley, A. E., Pettini, M., Reddy, N. A., & Adelberger, K. L. 2006b, *ApJ*, submitted
- [20] Ferreras, I., Wyse, R. F. G. & Silk, J. 2003, *MNRAS*, 345, 1381
- [21] Garnett, D. R., Bresolin, F., & Kennicutt, R. F. 2004, *ApJ*, 607, L21
- [22] Governato, F., Stinson, G., Wadsley, J., & Quinn, T. 2005, in *The Fabulous Destiny of Galaxies: Bridging Past and Present*, in press (astro-ph/0509263)
- [23] Hamann, F., Korista, K. T., Ferland, G. J., Warner, C., & Baldwin, J. 2002, *ApJ*, 564, 592
- [24] Ibata, R., Chapman, S., Ferguson, A.M.N., Lewis, G., Irwin, M., & Tanvir, N. 2005, *ApJ*, 634, 287
- [25] Kewley, L., & Kobulnicky, H. A. 2005, in *Starbursts: From 30 Doradus to Lyman Break Galaxies*, R. de Grijs & R. M. González Delgado eds., *ASSL Vol. 329*, (Dordrecht: Springer), 307
- [26] Kulkarni, V. P. & Fall, S. M. 2002, *ApJ*, 580, 732
- [27] Kulkarni, V. P., Fall, S. M., Lauroesch, J. T., York, D. G., Welty, D. E., Khare, P., & Truran, J. W. 2005, *ApJ*, 618, 68
- [28] Leitherer, C., Leão, J. R. S., Heckman, T. M., Lennon, D. J., Pettini, M., & Robert, C. 2001, *ApJ*, 550, 724
- [29] Leitherer, C., Schaerer, D., Goldader, J. D., Delgado, R. M. G., Robert, C., Kune, D. F., de Mello, D. F., Devost, D., & Heckman, T. M. 1999, *ApJS*, 123, 3
- [30] Madau, P., Ferguson, H. C., Dickinson, M. E., Giavalisco, M., Steidel, C. C., & Fruchter, A. 1996, *MNRAS*, 283, 1388
- [31] Maier, C., Lilly, S. J., & Carollo, C. M. 2005, in *The Fabulous Destiny of Galaxies: Bridging Past and Present*, in press (astro-ph/0509114)
- [32] Matteucci, F., & Pipino, A. 2002, *ApJ*, 569, L69
- [33] Matteucci, F., & Recchi, S. 2001, *ApJ*, 558, 351
- [34] Mehlert, D., et al. 2002, *A&A*, 393, 809
- [35] Mori, M., & Umemura, M. 2006, *Nature*, in press (astro-ph/0512424)
- [36] Naab, T., & Ostriker, J. P. 2006, *MNRAS*, 366, 899

- [37] Nagamine, K., Springel, V., & Hernquist, L. 2004, MNRAS, 348, 435
- [38] Navarro, J. F. 2004, in Penetrating Bars through Masks of Cosmic Dust, in press (astro-ph/0405497)
- [39] Nissen, P. E., Chen, Y. Q., Asplund, M., & Pettini, M. 2004, A&A, 415, 993
- [40] Pagel, B. E. J. 2002, in ASP Conf. Series 253, Chemical Enrichment of Intracluster and Intergalactic Medium, R. Fusco-Femiano, & F. Matteucci eds. (San Francisco: ASP), 489
- [41] Pagel, B. E. J., Edmunds, M. G., Blackwell, D. E., Chun, M. S., & Smith, G. 1979, MNRAS, 189, 95
- [42] Pagel, B. E. J., & Tautvaisiene, G. 1995, MNRAS, 276, 505
- [43] Pauldrach, A. W. A., Hoffmann, T. L., & Lennon, M. 2001, A&A, 375, 161
- [44] Pei, Y. C., & Fall, S. M. 1995, ApJ, 454, 69
- [45] Péroux, C., Dessauges-Zavadsky, M., D'Odorico, S., Sun Kim, T., & McMahon, R. G. 2005, MNRAS, 363, 479
- [46] Pettini, M. 2004, in Cosmochemistry: The Melting Pot of Elements, C. Esteban, A. Herrero, R. Garcia-Lopez, & F. Sanchez eds. (Cambridge: Cambridge University Press), 257 (astro-ph/0303272)
- [47] Pettini, M. 2005, in Astrophysics in the Far Ultraviolet, G. Sonneborn, H. W. Moos, & B. G Andersson eds. (San Francisco: ASP), in press (astro-ph/0601428)
- [48] Pettini, M., Boksenberg, A., & Hunstead, R. W. 1990, ApJ, 348, 48
- [49] Pettini, M., & Pagel, B. E. J. 2004, MNRAS, 348, L59
- [50] Pettini, M., Rix, S. A., Steidel, C. C., Adelberger, K. L., Hunt, M. P., & Shapley, A. E. 2002, ApJ, 569, 742
- [51] Prochaska, J. X., Herbert-Fort, S. & Wolfe, A. M. 2005, ApJ, 635, 123
- [52] Reddy, N. A., Erb, D. K., Steidel, C. C., Shapley, A. E., Adelberger, K. L., & Pettini, M. 2005, ApJ, 633, 748i
- [53] Reddy, N. A., & Steidel, C. C. 2004, ApJ, 603, L13
- [54] Reddy, N. A., Steidel, C. C., Fadda, D., Yan, L., Pettini, M., Shapley, A. E., Erb, D. K., & Adelberger, K. L. 2006, ApJ, in press (astro-ph/0602596)
- [55] Rix, S. A., Pettini, M., Leitherer, C., Bresolin, F., Kudritzki, R., & Steidel, C. C. 2004, ApJ, 615, 98
- [56] Savaglio, S., et al. 2004, ApJ, 602, 51
- [57] Savaglio, S., et al. 2005, ApJ, 635, 260
- [58] Schulte-Ladbeck, R. E., Rao, S. M., Drozdovsky, I. O., Turnshek, D. A., Nestor, D. B., & Pettini, M. 2004, ApJ, 600, 613
- [59] Shapley, A. E., Erb, D. K., Pettini, M., Steidel, C. C., & Adelberger, K. L. 2004, ApJ, 612, 108
- [60] Shapley, A. E., Steidel, C. C., Erb, D. K., Reddy, N. A., Adelberger, K. L., Pettini, M., Barmby, P., & Huang, J. 2005, 626, 698
- [61] Simcoe, R. A., Sargent, W. L. W., & Rauch, M. 2004, ApJ, 606, 92
- [62] Songaila, A. 2006, AJ, 131, 24
- [63] Stasińska, G. 2005, A&A, 434, 507
- [64] Steidel, C. C., Adelberger, K. L., Giavalisco, M., Dickinson, M., & Pettini, M. 1999, ApJ, 519, 1
- [65] Steidel, C. C., Adelberger, K. L., Shapley, A. E., Erb, D. K., Reddy, N. A., & Pettini, M. 2005, ApJ, 626, 44
- [66] Steidel, C. C., Giavalisco, M., Pettini, M., Dickinson, M., & Adelberger, K. L. 1996, ApJ, 462, L17
- [67] Steidel, C. C., Shapley, A. E., Pettini, M., Adelberger, K. L., Erb, D. K., Reddy, N. A., & Hunt, M. P. 2004, ApJ, 604, 534
- [68] Swinbank, A. M., Smail, I., Chapman, S. C., Blain, A. W., Ivison, R. J., & Keel, W. C. 2004, ApJ, 617, 64

- [69] Wild, V., Hewett, P. C., & Pettini, M. 2006, MNRAS, in press (astro-ph/0512042)
- [70] Wolfe, A. M., Gawiser, E., & Prochaska, J. X. 2003, ApJ, 593, 235
- [71] Wolfe, A. M., Prochaska, J. X., & Gawiser, E. 2005, ARAA, 43, 861
- [72] Wolfe, A. M., Turnshek, D. A., Smith, H. E., & Cohen, R. D. 1986, ApJS, 61, 249
- [73] Wyse, R. F. G., & Gilmore, G. 1995, AJ, 110, 2771
- [74] Zwaan, M. A., van der Hulst, J. M., Briggs, F. H., Verheijen, M. A., W., & Ryan-Weber, E. V. 2005, MNRAS, 364, 1467